Mineralogy and crystallography of vein metals in the Almahata Sitta ureilite. T. Mikouchi[1], C. A. Goodrich[2], V. Hoffmann[3,4], W. Satake[1], M. Kaliwoda[4,5], R. Hochleitner[4,5], A. M. Gigler[4,5], K. Sugiyama[6], and M. E. Zolensky[7], [1]Dept. of Earth and Planet. Sci., University of Tokyo, Hongo, Bunkyo-ku, Tokyo 113-0033, Japan (mikouchi@eps.s.u-tokyo.ac.jp), [2]Planet. Sci. Inst., Tucson, AZ 85719, USA, [3]Dept. of Geosci., University of Tübingen, 72076 Tübingen, Germany, [4]Dept. of Earth and Envir. Sci., University of München, 80333 München, Germany, [5]Mineral. State Collection, 80333 München, Germany, [6]Inst. for Materials Res., Tohoku University, Aoba-ku, Sendai, Miyagi 980-0812, Japan, [7]ARES, NASA Johnson Space Center, Houston, TX 77058, USA.

Introduction:

Almahata Sitta (AS) is possible fragments of asteroid 2008TC_3 which was detected still in space 19 hours before it hit the earth in October 2008 [1]. The mm-to-cm size fragments were recovered in Sudan (total ~10 kg) after the entry orbit was calculated and bright fireball was observed there [1]. The recovered fragments are mainly of ureilite lithologies showing variable mineralogy, but no obvious contact of different lithologies is observed [2]. Because of several pieces of evidence, it is considered that AS is a polymict breccia with loose connection of each fragment [1-2]. Fresh chondrite fragments were also recovered in the same strewn field, and they are considered as another fragment of 2008TC_3. These chondrite fragments consist of several different types including previously unknown group, but again no contact with different groups was found [e.g., 3,4].

The ureilite lithologies can be texturally divided into two types. One is a compact and coarse-grained lithology, and composed of large olivine and pigeonite grains (reaching mm in size) with interstitial graphite and Fe metal. This lithology is similar to typical ureilites. The other is porous and consists of fine-grained (10-20 μm in size) olivine and pyroxene with small amounts of metal and graphite [2,5].

Although Fe metal is commonly observed in all ureilite types, only limited works have been done on ureilite metals [e.g., 6-9]. In this abstract we report our ongoing mineralogical and crystallographic study of AS vein metals by using electron microprobe and electron back-scatter diffraction (EBSD) analysis with FEG-SEM [10].

Samples and Analytical Methods:

We studied polished sections of four different samples (AS #1, #7, #39, and #44). They were first characterized by optical microscope and FEG-SEM equipped with EDS (Hitachi S-4500 at University of Tokyo). Quantitative analysis was performed by JEOL JXA-8900L electron microprobe at University of Tokyo. The sections were then polished by colloidal silica to be analyzed by EBSD and obtained Kikuchi bands were calculated by using software developed by [11].

Results:

AS#1 and AS#7 show fine-grained textures and both large vein and small scattered Fe metal grains are present [2,5]. Although they show variable grain sizes (5-100 μm), they have narrow compositional ranges ($Fe_{0.92}Ni_{0.08}$-$Fe_{0.96}Ni_{0.04}$) with significant amount of Si and P (~2 and 0.4 wt%, respectively) in both samples. The obtained EBSD patterns could be indexed by *bcc* kamacite (α-Fe).

The samples #39 and #44 (AS#39 and AS#44) are typical coarse-grained ureilites and contain irregular-shaped vein metals (~500 μm long) at grain boundaries between silicate grains. The metals in AS#39 sometimes show rimming by Fe phosphide (schreibersite) [9]. The chemical composition of Fe metals in AS#39 show some variation (~1-4 wt% Ni and 0.2-4 wt% Si, respectively) [9], but all of them appear to be kamacite.

The vein metals in AS#44 are similar to those in AS#39, but closer look exhibits clear differences from AS#39, showing a large diversity of phase assemblages and textures [6,8,10]. The most common assemblage is intergrowth of two phases with apparent BEI contrast although the Fe content is same (Fig. 1). The brighter area has ~90 wt% Fe, ~6 wt% Ni, ~0.6 wt% Co, and ~3 wt% Si. The darker area has a slightly different composition with total of up to 93 wt%: ~90 wt% Fe, ~2 wt% Ni, ~0.3 wt% Co, and ~0.1 wt% Si. The darker area shows higher elevation in SEI as colloidal-silica polishing for EBSD produces clear relief surface in these areas, suggesting harder physical property of the darker phase. The EBSD analysis showed that the obtained Kikuchi bands of these darker areas in BEI match with the cohenite (Fe_3C) structure (Fig. 2). Although Fe metal is homogeneous in BEI, EBSD shows that small amounts of γ-iron (*fcc*) were present as well as kamacite (Fig. 2). The high contrast BEI shows that the brighter elongated phase (*bcc* iron) is present in the interstitial darker areas, corresponding to *fcc* iron (Fig. 3). Apart from these two iron phases and Fe carbide, Fe phosphide and Fe sulfide (troilite) are frequently found in all vein metals.

Discussions and Conclusions:

The co-existence of two iron phases (α and γ) with cohenite in AS#44 vein metal is unique and has not been found in other ureilites, but similar

occurrence can be found in commercial iron alloy [12]. In a simple Fe-C system, cohenite formed when the initial iron contains ≥0.77 wt% C. We consider that shock re-melting of pre-existing metal + graphite + sulfide + phosphide + silicide formed a eutectic-looking texture with variable present phases [10]. When the shock re-melting involved a large amount of graphite, cohenite formed as seen in Fig. 1 and 2. In contrast, when the graphite incorporation was small, only two iron phases formed by rapid cooling as seen in Fig. 3. Unfortunately, we cannot specify the peak temperature and their cooling rates because AS#44 metals contain different amounts of Fe-Ni-Co-S-Si-C-P and the phase diagram of such a complex system has not been well established.

Fe metals in AS#1 and AS#7 do not contain cohenite and γ-iron probably due to lower C content and slower cooling history compared with AS#44.

We plan to prepare FIB sections for TEM analysis to further characterize the vein metals in AS.

References:

[1] Jennsikens P. M. et al. (2009) *Nature*, *458*, 485-488. [2] Zolensky M. E. et al. (2010) *MAPS*, *45*, 1618-1637. [3] Bischoff A. et al. (2010) *MAPS*, *45*, 1638-1656. [4] Horstmann M. et al. (2010) *MAPS*, *45*, 1657-1667. [5] Mikouchi T. et al. (2010) *MAPS*, *45*, 1812-1820. [6] Goodrich C. A. et al. (2010) *MAPS*, *45*, A66. [7] Hoffmann V. H. et al. (2011) *MAPS*, *46* (in press). [8] Ross A. et al. (2011) *LPS XLII*, #2720. [9] Hochleitner R. et al. (2010) *Antarct. Meteorites*, *XXXIII*, 22-23. [10] Mikouchi T. et al. (2011) *MAPS*, *46*, A161. [11] Kogure T. (2003) *Jour. Crystal. Soc. Japan*, *45*, 391-395. [12] Smith W. F. and Hashemi J. (2006) Foundations of Materials Sci. & Eng., McGraw-Hill, pp. 1056.

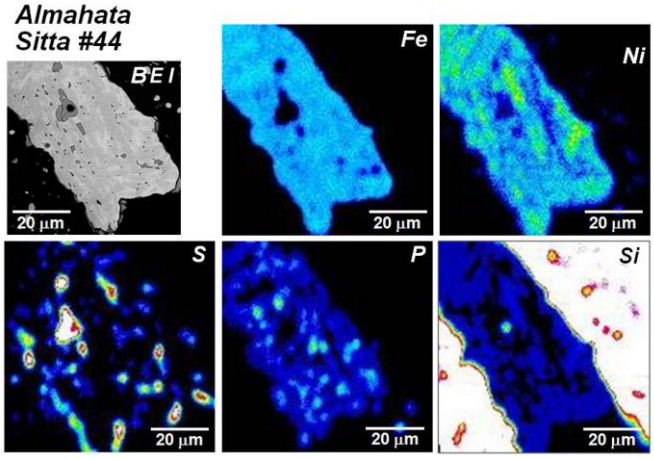

Fig. 1. BEI and X-ray maps of one of the vein metals in AS#44. Although BEI shows clear contrast, Fe abundance is nearly homogeneous. Brighter areas in BEI contrast contain more Ni and Si compared to darker areas. The EBSD analysis shows that darker areas are Fe carbide (Fig. 2). S and P X-ray maps show that both Fe sulfide and phosphide are scattered in the vein metal.

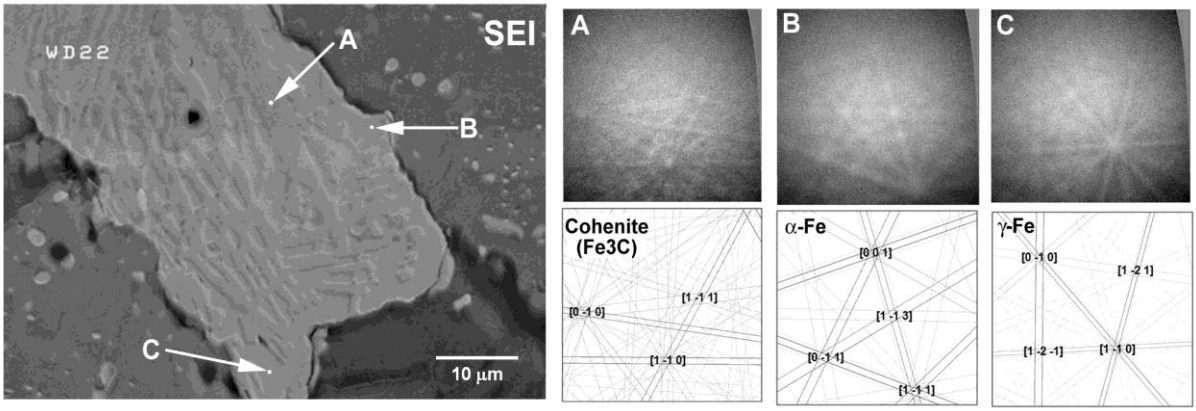

Fig. 2. SEI of one of the vein metals in AS#44 (same field of view of Fig. 1). The Kikuchi bands of three spots (A, B, and C in SEI) are shown in the right. The calculated patterns (below of A, B and C, respectively) showed that A is cohenite, B is *bcc* iron (α-phase), and C is *fcc* iron (γ-phase), respectively.

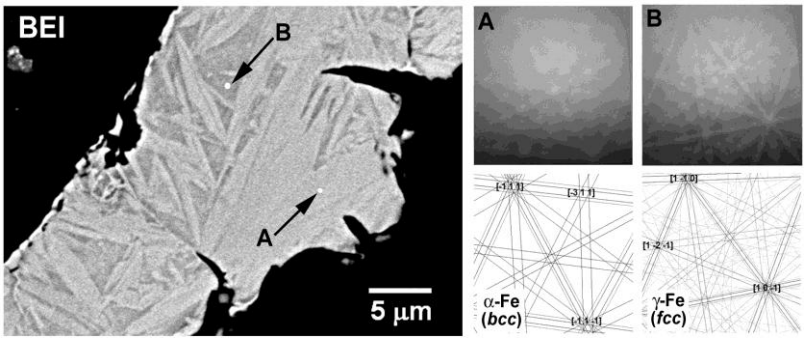

Fig. 3. High contrast BEI of one of the vein metals in AS#44 (different vein metal from Figs. 1 and 2). The Kikuchi bands of two spots (A and B in SEI) are shown in the right. The calculated patterns (below of A and B) showed that A is *bcc* iron (α-phase) and B is *fcc* iron (γ-phase), respectively.